Enhancement of hadron-electron discrimination in calorimeters by detection of the neutron component

O. Adriani[a], L. Bonechi[a], M. Bongi[b], S. Bottai[b], M. Calamai[c], G. Castellini[d], R. D'Alessandro[a], M. Grandi[b], P. Papini[b], S. Ricciarini[b], G. Sguazzoni[b], P. Sona[a], G. Sorichetti[e]

[a] *Università di Firenze and INFN-Firenze, Italy*
[b] *INFN-Firenze, Italy*
[c] *Università di Siena and INFN-Firenze, Italy*
[d] *IFAC-CNR,Firenze, Italy*
[e] *Università di Firenze, Italy*

Abstract

In many physics experiments where calorimeters are employed, the requirement of an accurate energy measurement is accompanied by the requirement of very high hadron-electron discrimination power. Normally the latter requirement is achieved by designing a high-granularity detector with sufficient depth so that the showers can fully develop. This method has many drawbacks ranging from the high number of electronic channels to the high mass of the detector itself. Some of these drawbacks may in fact severely limit the deployment of such a detector in many experiments, most notably in space-based ones. Another method, proposed by our group and currently under investigation, relies on the use of scintillation detectors which are sensitive to the neutron component of the hadron showers. Here a review of the current status will be presented starting with the simulations performed both with GEANT4 and FLUKA. A small prototype detector has been built and has been tested in a high-energy pion/electron beam behind a "shallow" calorimeter. Results are encouraging and indicate that it is possible to enhance the discrimination power of an existing calorimeter by the addition of a small-mass neutron detector, thus paving the way for better performing astroparticle experiments.

Key words: Calorimetry, neutron detection, astro particle, space experiments

1. Introduction: neutron production in calorimeter showers

Following the spectacular results of the Pamela [1] experiment, which relied on the experiment's exceptional hadron rejection power, it was decided by a group of researchers from Florence to further pursue the investigation in the use of neutron detectors coupled to shallow calorimeters. In fact the Pamela experiment itself already uses a traditional ^{3}He detector as a neutron catcher at the bottom of the calorimeter. Although it is sensitive only to thermalized neutrons and has very low efficiency, it has been used for checking systematics and for efficiency measurements. Thus detailed simulations were performed to determine the neutron component of different types of calorimetric showers, with a real case in hand, namely the CALET proposal for the International Space Station [2]. This is a next generation electromagnetic calorimeter, designed with the aim of accurately measuring the electron spectra in primary cosmic rays. The two calorimeter components are shown in Fig. 1.

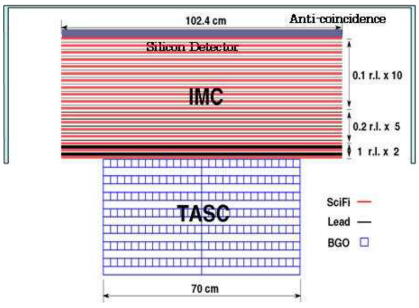

Figure 1: The CALET calorimeters. On top the IMC with less than 2 radiation lengths. The TASC (33 X_0) completely absorbs the electron shower.

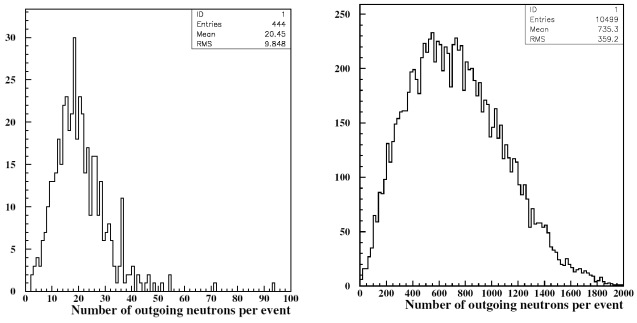

Figure 2: Neutrons produced by 400 GeV electron (left) and 1 TeV proton (right) showering in the CALET calorimeters (FLUKA simulation).

The simulations [3] compared neutrons exiting from the bottom of the calorimeter for two typical scenarios: one using

400 GeV electrons, the other using 1 TeV protons with the additional requirement that they interact in the IMC part. In this way the two types of particle release the same energy in the TASC part. The results show a large difference in the quantity of neutrons produced in the two cases as shown in Fig. 2. This is only to be expected since in hadronic showers neutrons can be produced by nuclear excitation, spallation and the giant resonance mechanism, while only the latter is active in electromagnetic showers. In addition the neutron spectra is harder in the case of hadronic showers, while time of arrival, in both cases, coincides with the charged particle shower core but has a significant tail lasting up to a few microseconds (see Fig. 3). Thus a fast detector sensitive to neutrons and with good time resolution, placed at the end of a shallow calorimeter, could in principle help in discriminating between hadronic and electromagnetic showers just by counting the number of neutrons present.

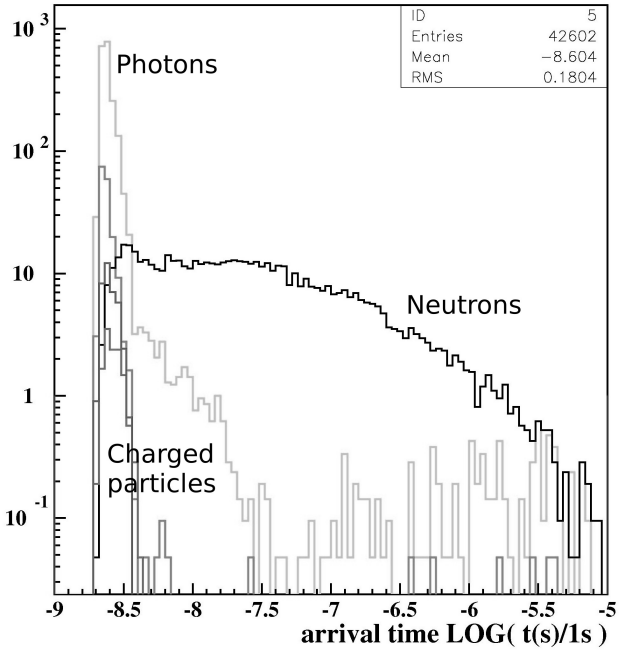

Figure 3: Shower particles time of exit (zero time is 1 ns) at the bottom of the calorimeter. In black neutrons, light gray photons, while other shades are charged particles (FLUKA).

2. The Neucal detector

Following the above mentioned simulation results, it was decided to build an "active" moderator type detector, where plastic scintillators would not only provide neutron moderation but also give fast light signals whenever the neutron interacted. Simulations were performed concerning number and thickness of layers and lateral extension of the detector. For example from Fig. 4 it is evident that while 100 keV neutrons effectively interact in the first 2-3 scintillator layers, more layers are needed to be able to detect 10 MeV or even more energetic neutrons. The lateral dimensions of the detector were chosen by observing that neutrons from the showers interact mostly within a radius of 20 cm from the shower centre, as shown in Fig. 5 for 10-MeV neutrons.

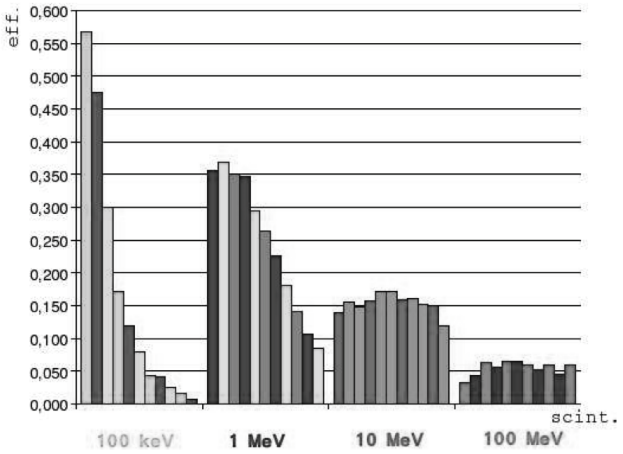

Figure 4: Detection efficiency for neutrons of various energies, as a function of scintillator layer number (1 cm thickness). Simulated data (FLUKA).

Once the physical dimensions were defined, the following criteria were also taken into account in the design of the detector:

1) Almost all neutrons exit from the calorimeter within a few microseconds but thermalization inside the neutron detector can take hundreds of microseconds. So fast photomultiplier tubes (Hamamatsu R5946) and flash digitizer boards capable of storing 1 millisecond or more of sampled data were used for the readout.

2) Complement the scintillator part with ^{3}He tubes for redundancy and cross checks.

3) Use of a modular structure with the possibility of inserting thin lead foils to augment the detector neutron sensitivity.

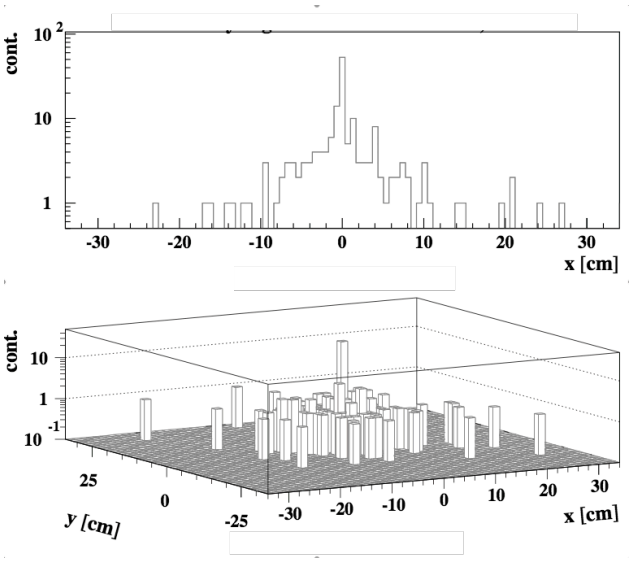

Figure 5: Lateral spread of the energy deposits in the 9^{th} scintillator plane of the Neucal detector, produced by 10 MeV neutrons exiting the calorimeter. Simulated data (FLUKA).

The final design is shown in Fig. 6. It consists of nine iden-

tical modules stacked in a three by three matrix. Each module itself consists of three EJ220 scintillator plates of 1 cm thickness, coupled through a common light guide to the R5946 photomultiplier.

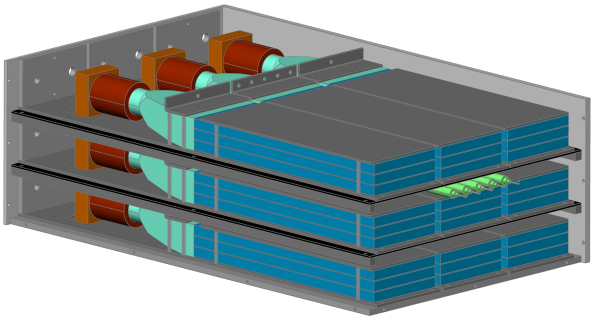

Figure 6: Schematic drawing of the Neucal detector. Apart from the scintillator stacks (blue) described in the text, five ^{3}He tubes (green) are lodged at the centre of the detector.

The first prototype [4] was built in our laboratory in Florence and is shown in Fig. 7. From the start it was decided that the material and components used would be reused many times. Thus no glue was used, only optical grease, so as to better rearrange all components, depending on the outcome of the test beams and simulations. The assembly of nine identical bricks was then placed in a light-tight aluminum box with three drawers. The nine light guides inside the drawers were not wrapped and

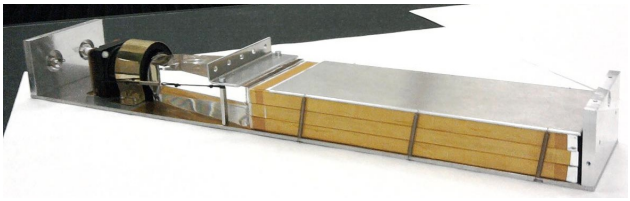

Figure 7: Photo of one of the nine scintillator bricks. The three scintillator plates are individually wrapped and are $25 \times 8 \times 1$ cm^3 (LWH). A single light guide channels the photons to the photomultiplier held in place with a simple collar.

thus some light leakage was found when examining the shower events. Five ^{3}He tubes (Canberra 12NH25/1) were also placed at the middle of the detector.

The nine scintillators and five tubes were read out by fast digitizer boards capable of recording up to 10 ms worth of data samples. Two modules were used, one a CAEN V1731 with 500 MS/s capability but only 8 bit range, the other a CAEN V1720 with a more limited 250 MS/s capability but 12 bit range. Each board has 8 input channels. Seven of the nine scintillator signals plus the coincidence trigger were sent to the 500 MS/s board, while the two remaining scintillator signals and the five ^{3}He tubes plus again the coincidence trigger were sent to the 250 MS/s module. The readout was performed with a VME system.

3. Test beam

A test was performed at CERN SPS, line H4 (one week test). The Neucal detector was placed behind a shallow calorimeter consisting of tungsten plates for a total of 16 X_0 lengths. Data was collected for pions (350 GeV), electrons (100-150 GeV) and muons (150 GeV). During the pion runs more absorber was placed in front of the calorimeter bringing the number of radiation lengths up to 29.

3.1. Signal views

Data was taken mostly in zero suppression mode in order to reduce both the event size and the readout time. The "movie"

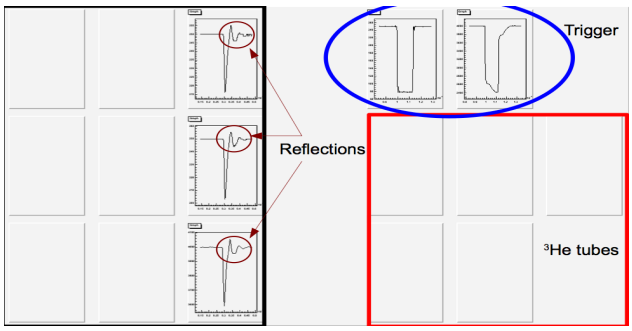

Figure 8: A graphical representation of the digitizer channels. To the left the nine scintillator bricks, to the right the triggers and the five ^{3}He tubes. A muon signal appears in coincidence on the three rightmost scintillator bricks. Particles enter from the top.

was then reconstructed offline and a search was performed for delayed signals arriving up to hundreds of microseconds after the initial charge particle shower. In general, a neutron inter-

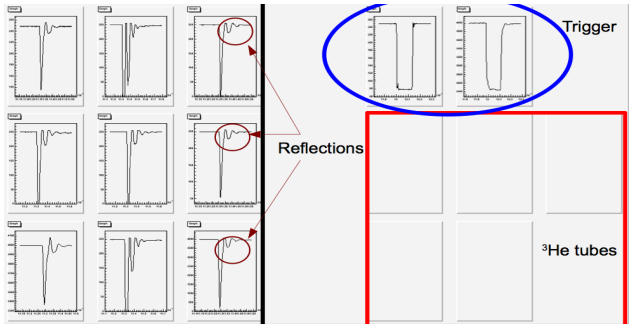

Figure 9: Using the same layout as in Fig. 8. An electron shower appears in coincidence on all scintillator bricks. No other signals were observed at subsequent times.

action is expected to show as an isolated energy deposit in one of the scintillator bricks or ^{3}He tubes, while a traversing hadron or charged particle will release energy on more than one brick. An example of this is shown Fig. 8 (muon traversing the detector), Fig. 9 (electron shower) and Fig. 10 (pion shower). In the latter, isolated signals appear both in the scintillator bricks and the ^{3}He tubes.

The reflections seen in the reconstructed digitizer output last for a few hundred nanoseconds and effectively spoil the data in

Figure 10: Using the same layout as in Fig. 8. A pion shower appears in coincidence on all scintillator bricks. Also other isolated signals appear as the film unrolls both on some scintillator bricks and on one ^{3}He tube.

the short time windows around the shower core. Unfortunately this was an artifact introduced by our hardware during zero suppression mode, which has now been corrected. Most of the data taken was in this mode and cannot be used to analyze this time window. Unfortunately also the few ten thousand events taken without zero suppression suffer from saturation effects due to the limited ADC range (8 bits), and this has severely limited our short time delay analysis.

3.2. Results

A comparison was made with a GEANT4 based simulation of the test beam layout. Data in the plots (see Fig. 11 and Fig. 12) are limited to after 1 μs after the shower core because of the reflection artifacts. The energy scale was normalized to the muon data.

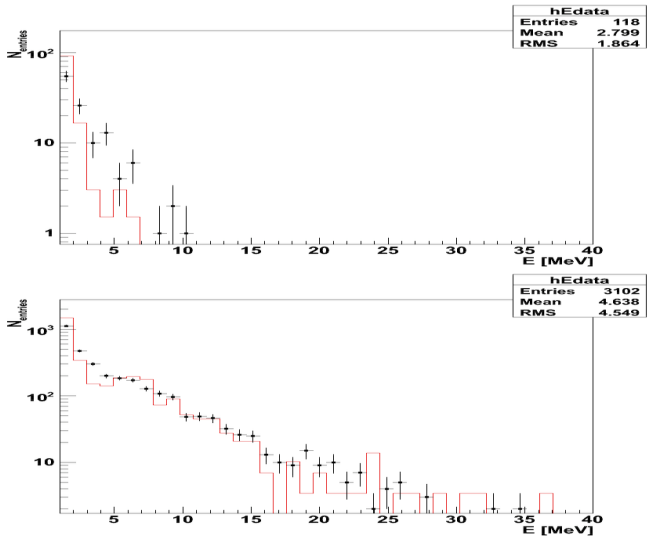

Figure 11: Top: energy spectra of signals seen in Neucal after 1μs for 33000 electron triggers. Bottom: energy spectra of signals seen in Neucal after 1μs for 75000 pion triggers, of which roughly a third have interacted. The solid red lines show the predictions of the Geant4 simulation.

The very few events (order of 10000) taken without zero suppression were also analyzed to extract neutron data in the time interval before 1 μs. Only the two lateral scintillator bricks which had been read out with the slower 12 bit ADCs provided

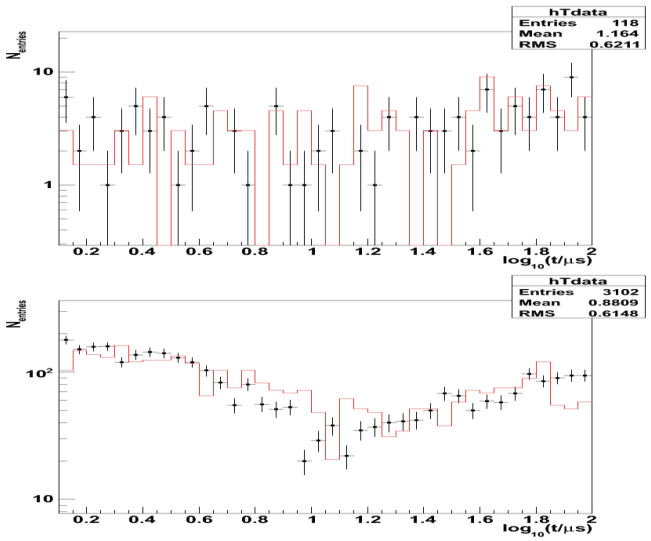

Figure 12: Top: time spectra of signals seen in Neucal after 1μs for 33000 electron triggers. Bottom: energy spectra of signals seen in Neucal after 1μs for 75000 pion triggers, of which roughly a third have interacted. The solid red lines show the predictions of the Geant4 simulation.

meaningful data. This time the problem was not with reflections but with saturation and recovery time of the ADC module itself. Again (see Fig. 13) there is a marked difference in the quantity of signals seen for electromagnetic and hadronic showers. The actually interacting pions in our data in these conditions amount only to 1645 events, which are compared with the same number of electromagnetic showers.

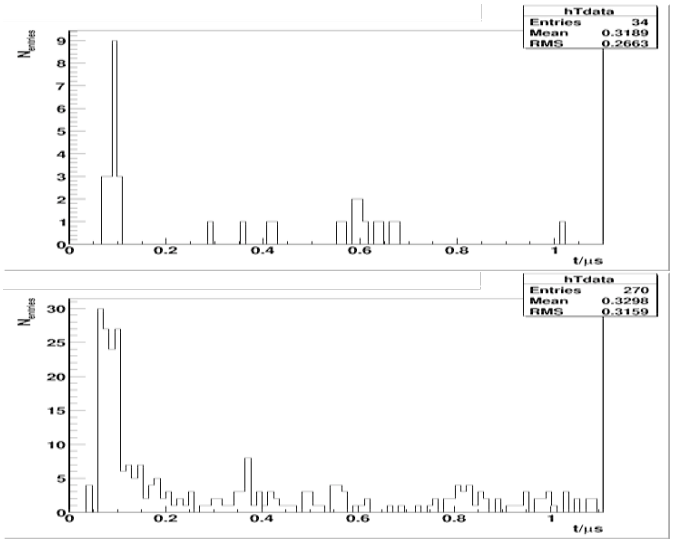

Figure 13: Top: time spectra of signals seen in Neucal in a 1 μs window after the end of the shower core for electron showers. Bottom: energy spectra in the same conditions but for interacting pion showers.

4. Conclusions

A new approach to hadron/electron separation is being pursued. Advantages are the possibility of achieving the same per-

formance in terms of hadron rejection power with lighter, more compact calorimeters. Results are very encouraging and entice us to repeat the tests with more adequate electronics and with better calorimeter control.

Data were also taken at the end of 2009 at the nTOF [5] facility at CERN. The analysis is still ongoing and aims at measuring the efficiency of the detector as a function of neutron energy.

References

[1] O. Adriani et al., Nature 458 (2009) 607.

[2] S. Torii et al., Nuclear Physics B - Proceedings Supplements Volume 166, April 2007, Pages 43-49.

[3] S. Bottai, et al., Nucl. Instr. and Meth. A (2009), doi:10.1016/j.nima.2009.10.089

[4] L. Bonechi et al., ICATPP09 presentation at Villa Olmo, Italy.

[5] The nTOF Collaboration, Proposal for a Neutron Time Of Flight Facility, CERN/SPSC 99-8, SPSC/P 310 (1998).